ARTICLE IN PRESS

Nature Communications

https://doi.org/10.1038/s41467-026-70857-7

Article in Press

One-step fabrication of superhydrophobic fabrics with stable mechanical performance in harsh conditions

Received: 23 July 2025

Accepted: 3 March 2026

Cite this article as: Liu, Z., Zhao, K., Ma, J. *et al.* One-step fabrication of superhydrophobic fabrics with stable mechanical performance in harsh conditions. *Nat Commun* (2026). https://doi.org/10.1038/s41467-026-70857-7

Zhuoxing Liu 刘卓星, Kexin Zhao 柯心, Jie Ma , Shijie Liu 刘士杰, Zidong Zhan 展梓 , Cunlong Yu 于存 , Lei Wu 吴磊, Dezhao Hao 郝德昭, Lei Jiang 江雷 & Zhichao Dong 董智超

We are providing an unedited version of this manuscript to give early access to its findings. Before final publication, the manuscript will undergo further editing. Please note there may be errors present which affect the content, and all legal disclaimers apply.

If this paper is publishing under a Transparent Peer Review model then Peer Review reports will publish with the final article.

ARTICLE IN PRESS

© The Author(s) 2026. **Open Access** This article is licensed under a Creative Commons Attribution-NonCommercial-NoDerivatives 4.0 International License, which permits any non-commercial use, sharing, distribution and reproduction in any medium or format, as long as you give appropriate credit to the original author(s) and the source, provide a link to the Creative Commons licence, and indicate if you modified the licensed material. You do not have permission under this licence to share adapted material derived from this article or parts of it. The images or other third party material in this article are included in the article's Creative Commons licence, unless indicated otherwise in a credit line to the material. If material is not included in the article's Creative Commons licence and your intended use is not permitted by statutory regulation or exceeds the permitted use, you will need to obtain permission directly from the copyright holder. To view a copy of this licence, visit http://creativecommons.org/licenses/by-nc-nd/4.0/.

Title

One-Step Fabrication of Superhydrophobic Fabrics with Stable Mechanical Performance in Harsh Conditions

Author list

Zhuoxing Liu(刘卓星)[1,2], Kexin Zhao(赵柯心)[1,2], Jie Ma(马洁)[1,2], Shijie Liu(刘士杰)[3,4], Zidong Zhan(展梓栋)[1,2], Cunlong Yu(于存龙)[1], Lei Wu(吴磊)[5*], Dezhao Hao(郝德昭)[1,2*], Lei Jiang(江雷)[1,4], and Zhichao Dong(董智超)[1,2,3,4*]

Affiliations

[1]Laboratory of Bio-Inspired Smart Interface Science, Technical Institute of Physics and Chemistry, Chinese Academy of Sciences, Beijing 100190, China.

[2]School of Future Technology, University of Chinese Academy of Sciences; Beijing 100049, China.

[3]State Key Laboratory of Bioinspired Interfacial Materials Science, Suzhou Institute for Advanced Research, University of Science and Technology of China, Suzhou, Jiangsu 215123, China.

[4]School of Chemistry and Materials Science, University of Science and Technology of China, Hefei, Anhui 230026, China.

[5]Key Laboratory of Green Printing, Beijing National Laboratory for Molecular Sciences (BNLMS), Institute of Chemistry, Chinese Academy of Sciences, Beijing, 100190, China.

Corresponding author:

Lei Wu, wulei1989@iccas.ac.cn

Dezhao Hao, haodezhao@mail.ipc.ac.cn

Zhichao Dong, dongzhichao@mail.ipc.ac.cn

Abstract

Developing robust water-repellent textiles is critical for outdoor, protective, and industrial applications. However, achieving long-lasting water repellency under mechanical stress remains a significant challenge. Conventional approaches typically rely on nanoparticle assemblies or PFAS-based finishes, which often detach or degrade when subjected to abrasion or harsh conditions. Here, we demonstrate a molecularly assembled robust superhydrophobic shell (MARS) technique that directly constructs an ordered, covalently bonded, fluorine-free silica shell on individual yarn fibers via a one-step process. MARS eliminates the need for discrete nanoparticles or fluorinated chemistries and is compatible with a wide range of natural and synthetic fibers. This fiber-level treatment maintains superhydrophobicity even after the fibers are woven or knitted into finished textiles, while preserving breathability and mechanical resilience. MARS combines biomimetic inspiration with practical, scalable fabrication to meet urgent performance needs. Unlike conventional coatings that progressively degrade, the permanently bonded MARS coating endures intensive abrasion, high-velocity water impacts, steam exposure, and extreme temperature cycles. By addressing key challenges such as PFAS restrictions and the fragility of traditional coatings, the MARS method paves the way for next-generation water-repellent fabrics that balance sustainability and high performance across outdoor, protective, medical, and industrial applications.

Introduction

Superhydrophobic fabrics are designed to repel water, resist staining, and remain lightweight and breathable in demanding applications[1]. Depositing fluorinated compounds nanoparticle coatings[2–5], silicone nanofilament[6, 7] coatings or silane-based interpenetrating networks on various textiles[6-8] can achieve superhydrophobicity, initially providing effective water repellency[3,9]. However, such treatments lack long-term durability, as the weak adhesion between particles makes them prone to abrasion and fabric deformation[4]. Moreover, nanoparticle layers can seal the interstitial pores of fabrics[5, 9, 10], which increases weight[11], diminishes breathability, and adversely affects the fabric's hand and drape, limiting their suitability for lightweight, durable outdoor garments[1]. Environmental and health concerns further complicate the reliance on fluorinated finishes[12]. Regulatory restrictions against per- and polyfluoroalkyl substances (PFASs) have intensified due to their environmental persistence, potential toxicity, and associated health risks[13], prompting the textile industry to seek sustainable, non-fluorinated alternatives that offer comparable durability[14].

Biomimetic inspiration offers a path forward[15]. Lotus leaves[16,17], Salvinia leaves[18], insect wings[19], penguin feathers[20], and the cuticles of soil-dwelling springtails[21, 22] exhibit fluorine-free superhydrophobicity in nature. Springtails, tiny soil-dwelling arthropods, offer a remarkable example through their in-situ superhydrophobic skin[23], which enables survival in wet, abrasive environments (Fig. 1a). The springtail's skin combines mushroom-shaped microstructures and nanoscopic ridges to repel water[21], prevent contamination[22], and resist mechanical damage[23] (Fig. 1b). This natural design has inspired robust coatings on rigid substrates[15, 24, 25], but translating such micro–nano architectures to flexible, breathable textiles has remained challenging.

Motivated by the springtail cuticle and the pressing need for sustainable water-repellent fabrics, we developed an in-situ molecularly assembled robust-superhydrophobic shell (MARS) technique that covalently anchors a carbon-chain silane/SiO_2 network directly onto fiber surfaces through a one-step molecular assembly, creating continuous superhydrophobic shells at the fiber level without the need for discrete nanoparticles. Incorporating long-chain alkyl silanes into the silica matrix yields an interpenetrating, crosslinked network that retains hydrophobicity under severe abrasion, high-pressure water jets, and steam exposure. By treating fibers before textile formation, MARS endows both yarns and the resulting fabrics with permanently bonded, fluorine-free superhydrophobicity while maintaining breathability, tensile strength, and flexibility.

Results

Molecular assembly robust superhydrophobic shell on fiber

The MARS modification process involves continuously coating twisted yarns with a fluorine-free solution that reacts rapidly in humid air to form a covalently bonded, nanostructured silica shell functionalized with long alkane chains (Fig. 1c). The process begins by passing twisted yarns (150D, 36F; yarn radius ~150 μm; single-fiber diameter ~10 μm) through a petroleum ether solution (boiling point 30-60°C) containing 4% (*w*/*v*) tetrachlorosilane (TCS) and 2% (*w*/*v*) octadecyltrichlorosilane (OTS) at a linear speed U of 0.25 $\mathrm{m{\cdot}s^{-1}}$ (Supplementary Fig. 1, Supplementary Movie 1). MARS utilizes low-cost raw materials and a simple, energy-efficient process. TCS and OTS are industrially available silanes. TCS is a byproduct of high-purity silicon production and serves as a key raw material in the silicon and rubber industries[26]. Additionally, TCS can be recycled from silicone waste, offering a cost-effective solution with high recycling potential[27]. TCS, with its lower steric hindrance, reacts more rapidly with the hydroxyl groups in cellulose-based natural fibers[28] (e.g., cotton, linen; see Supplementary Fig. 2). The low viscosity ($\eta \approx 0.3$ mPa·s) and surface tension ($\gamma \approx 24.3$ $\mathrm{mN{\cdot}m^{-1}}$) of the carrier solvent yield a capillary number $Ca = \eta U/\gamma \sim 10^{-3}$, entraining a uniform liquid film of thickness $e = 1.37\, d\, Ca^{2/3}$ (on the order of 100 μm, where d is the yarn diameter)[29]. This coating corresponds to a modest increase in yarn mass of approximately 6.1%. Additionally, the use of petroleum ether enables solvent recycling during condensation, enhancing fabrication efficiency. Based on our estimates, treating a 170 g cotton fabric (1 $\mathrm{m^2}$) costs only about \$0.27 (roughly \$1.56 per kg of fabric), which can be reduced to ~\$0.12 (~\$0.69 per kg) if ~75% of the solvent is recovered, indicating that the MARS treatment is economically feasible for large-scale manufacturing.

Within seconds of exiting the bath, the solvent evaporates (Supplementary Fig. 3), and ambient moisture hydrolyzes TCS (owing to its smaller molecular size compared to OTS)[30], preferentially undergoes rapid hydrolysis and condensation to form an amorphous SiO_2 network covalently grafted to available –OH groups on natural fibers (Supplementary Fig. 2). Subsequently, OTS reacts at the newly formed silica surface, anchoring C_{18} alkyl chains that dramatically lower the surface energy[31], analogous to plant wax layers[16,17], without the need for perfluorinated reagents[12] (Supplementary Fig. 4). The resulting architecture on yarns comprises 36 individual fibers (~10 μm diameter each) with mushroom-like silica aggregates (130-170 nm in diameter) and tightly adhered silica shells (20-50 nm feature size) on their surfaces (Fig. 1d, Supplementary Fig. 5), demonstrating a hierarchical coating structure. On synthetic substrates lacking native hydroxyl groups (e.g., polyester, nylon), the low-polarity, small-molecule TCS penetrates slightly into the fiber surface, where it crosslinks in situ to anchor the amorphous SiO_2 network onto the fibers, ensuring broad material compatibility (Supplementary Fig. 5). This sequential, self-separating reaction yields a distinct shell nanostructure (Supplementary Fig. 5). The TCS-derived silica forms a robust inner skeleton covalently bonded to the fiber surface, while OTS forms an outer hydrophobic layer (Supplementary Fig. 6). We hypothesize that this covalently integrated core–shell architecture is key to the coating's exceptional mechanical durability.

Next, we evaluated superhydrophobicity at the single-fiber scale using a contact angle tensiometer[32] equipped with a 20× magnification lens. Even 20 pL droplets (~30 μm diameter) exhibited an apparent contact angle θ_a of 160.0° on individual cotton fibers (Fig. 1e). Wool, polyester, and nylon fibers all demonstrated superhydrophobic behavior, with θ_a values of 157.6°, 163.0°, and 156.5°, respectively (Supplementary Fig. 7). Environmental scanning electron microscopy at 3.7°C and 100% relative humidity[33] further revealed that a condensing microdroplet (<2 μm diameter, ~6 fL) on a single fiber will roll off once it grows to ~2 μm in size, demonstrating excellent water repellency even under cool, saturated conditions (Fig. 1f).

Finally, MARS-modified yarns were fabricated into woven and knitted textiles and even used to embroider superhydrophobic motifs onto untreated fabrics (Fig. 1g-i). The MARS-textiles exhibited high apparent water contact angles of 154.7° (woven) and 156.1° (knitted) (Fig. 1g, h), as well as ultralow sliding angles of 1.8° and 3.0°, respectively. The droplet rests only on the texture tips, with air trapped in the hollows beneath, forming a Cassie–Baxter state[34] (Fig. 1h, Supplementary Movie 2), which prevents water from penetrating into the fabric. The observed Cassie–Baxter superhydrophobicity is attributed to the textiles' three-tier hierarchical milli-/micro-/nanostructures[35], a dense yet rough surface texture at the nanoscale[2, 9], and the low surface energy imparted by the alkyl-silane modification (Fig. 1d, h). Moreover, embroidered patterns in multiple colors (light/dark green and pink) maintained $\theta_a \approx 161.5°$ on a lotus-flower motif, whereas the surrounding untreated fabric readily absorbed dyed water (Fig. 1i). Across all color variants, ΔE^* color shifts[36] remained below 1.0, indicating that the thin silica shells preserve the original hues and protect fibers from mechanical stresses during weaving, knitting, and embroidery (Supplementary Fig. 8).

Water-repellent evaluation of MARS-modified fibers

We applied the MARS modification to everyday apparel items. A white T-shirt, black leggings, and a white shoe vamp (upper) (Fig. 2a, Supplementary Fig. 9) and compared their water-repellency against fabrics coated by conventional spray-on treatments (Ultra-Ever Dry and a Capstone ST-200 + fused silica mixture) (Fig. 2a). In a continuous water-impact spray test (based on AATCC 22)[37], MARS-modified fabrics withstood over 25 liters of water sprayed before any wetting occurred, surpassing the standard 250 mL-per-impulse benchmark by a factor of 100 and achieving the highest AATCC spray rating of 100 (Fig. 2b, Supplementary Movie 3). Similar resistance was observed against various common liquids, including beverages and carbonated soft drinks, demonstrating robust repellency under real-world spill conditions (Supplementary Fig. 10a). Significantly, the water repellency was retained across a broad spectrum of textile substrates, including natural fabrics (linen, cotton, wool) and synthetics (spandex, nylon, acetate, polyester), highlighting the versatility of the MARS modification process (Supplementary Fig. 10b).

Under millimeter-scale water droplet impacts (25°C, Weber number ~5.4), individual drops consistently bounced off the fabric surface up to six times (Fig. 2c). In simulated heavy rain tests, the MARS-modified fabric resisted 12 hours of continuous raindrop impacts, withstanding over 10^4 impacts at a single point (2.5 drops per second, impact velocity 2.4-3.0 $\mathrm{m{\cdot}s^{-1}}$) (Fig. 2d, Supplementary Fig. 11a-c). To further challenge the coating's resistance to high-speed water, we designed a rotational-jet impact setup (Supplementary Fig. 11d, e, Supplementary Movie 3). Whereas conventional superhydrophobic coatings failed when impacted by droplets at 5.0-6.6 $\mathrm{m{\cdot}s^{-1}}$, the MARS-modified fabrics effectively repelled water drops impacting at 11.6 $\mathrm{m{\cdot}s^{-1}}$, equivalent to the velocity of a raindrop during a 100-meter sprint (Fig. 2e).

In the Bundesmann rain-shower test, which subjects textiles to kinetic energies far exceeding those of natural downpours (~5.8× a cloudburst, 90× heavy rain, 480× moderate rain, 21,000× light rain)[38], a canvas fabric spray-coated with Capstone-FS lost its repellency, receiving an AATCC score of 50 (~70% of its surface wetting) and allowing 243.7 mL of water to penetrate. In stark contrast, the MARS-modified canvas achieved an AATCC score of 100 with only 1.7% water absorption and almost no water penetration (Fig. 2f, Supplementary Fig. 12). Moreover, under standard machine laundering with detergent[2,37], MARS-modified fabrics retained their superhydrophobic performance, scoring AATCC 100 after five wash cycles and AATCC 95 after twenty cycles, with static contact angles remaining above 150° throughout (Supplementary Table 1).

Durability and Wear Resistance

Every day use always involves rubbing against sleeves or backpack straps, or repeated handling of garments, which subjects textiles to abrasion, peeling, and stretching that can easily damage the fine micro- and nano-structures or weakly bound layers responsible for water repellency[1,4,5]. To evaluate the practical wear resistance of MARS, we conducted both standardized laboratory abrasion tests and application-specific simulations, including Martindale and Taber abrasion tests, falling-sand impact, vibration, stretching, peeling, scrubbing, and treadmill running.

In the Martindale test, MARS-treated canvas fabric endured up to 80,000 abrasion cycles against a standard wool fabric under 9 kPa pressure while maintaining a $\theta_a > 150°$ and minimal contact angle variation ($\Delta\theta < 5°$) (Fig. 3a, Supplementary Movie 4). Unlike conventional coatings that degrade after only a few hundred cycles[1,4], the MARS-modified fabrics demonstrated exceptional durability. Notably, in the more aggressive Taber test (a 250 g load for 20,000 cycles), the MARS-treated fabrics retained superhydrophobicity ($\theta_a \approx 156.7°$) with a slight apparent contact angle drop ($\Delta\theta \approx 8.8°$). In the Taber test, SEM images (Supplementary Fig. 13, inset) confirm that even after 20,000 abrasion cycles, the nanostructured MARS shell remains intact on the fiber surface, providing direct visual evidence of the coating's robustness.

Compared with previous durable superhydrophobic treatments, such as silicone nanofilament coatings[6, 7, 39], silica nanoparticles[40] and perovskite-silane composite fibers[8], the covalent bonding of MARS offers a distinct advantage in mechanical robustness. Silicone nanofilaments typically adhere to fibers via physical entanglement or physisorption. In contrast, MARS forms a molecularly assembled interpenetrating network shell that is chemically grafted to each fiber's surface (Supplementary Fig. 4). The nanostructured silica shells, securely embedded within the fiber matrix, significantly outperformed conventional nanoparticle-based coatings, with a reduced abrasion depth of 46.2% (Fig. 3b, Supplementary Fig. 13, Supplementary Movie 4). In falling sand tests[1,37], where impacts from quartz sand abrade fabrics, MARS-treated samples withstood 100 cycles of implications from a total of 320 kg of sand while maintaining their water-repellent properties (Fig. 3c).

We assessed the effect of the MARS coating on the textile's tactile properties, as coating processes often compromise fabric feel. As shown by quantitative fabric hand measurements (Fig. 3d and Supplementary Table 2), the MARS-treated fabric is virtually indistinguishable from the untreated control in key haptic metrics such as bending rigidity and surface roughness (e.g., 31.7 gf·mm/rad vs. 31.1 for control; surface roughness ~7.6 µm vs ~7.4 µm for control). This provides strong evidence that MARS's ultrathin coating imparts robust functionality without sacrificing the fabric's natural softness, drape, or breathability, unlike many conventional coatings that stiffen the textile.

To simulate real-life wear under motion, MARS-treated fabrics were integrated into garments and subjected to various usage scenarios. A MARS-treated T-shirt was worn during a 1-hour treadmill run with a backpack (Fig. 3e), where the shoulder straps caused frictional oscillatory motion similar to that experienced during running and jogging[41]. In a mimetic vibration test (harmonic shoulder-strap rubbing at 2 Hz, 2 mm amplitude), the coating withstood over 600,000 friction cycles with no significant loss of superhydrophobicity (Fig. 3f). In addition, a knitted MARS fabric retained superhydrophobicity after 20,000 stretch cycles, surviving extensive fiber-to-fiber abrasion (Fig. 3g). For practical footwear, MARS-modified shoe uppers endured 8,000 brushing strokes (simulating vigorous cleaning) with negligible pilling or change in water repellency ($\Delta\theta < 3.2°$) (Fig. 3h, Supplementary Movie 4). Even after 500 cycles of 3M tape peeling at 90°, the MARS fabric's θ_a remained ~155° ($\Delta\theta \approx 9.1°$) (Fig. 3i, Supplementary Fig. 14).

Beyond apparel, we tested MARS-treated socks under sustained load. A wearer ran 15,000 steps on a treadmill, exerting ~51.3 kPa pressure per step (Fig. 3j). Conventionally treated socks (Capstone-FS) showed visible white residue from coating abrasion and lost water repellency (contact angle dropped to ~139.7°). In contrast, MARS-treated socks maintained their water-repellent properties without noticeable degradation ($\Delta\theta$ only ~1.7°) (Fig. 3k, Supplementary Movie 4). Finally, to assess long-term outdoor performance, MARS-modified fabrics were exposed to the natural environment for 360 days (Supplementary Fig. 15a), spanning all seasons and including high solar radiation, sandstorms, rain, frost, and icing (temperatures from -16.8 to 41.2°C; humidity 9% to 100%). Supplementary Fig. 15b summarizes the temperature, rainfall, and light conditions during this year-long exposure. A MARS-modified T-shirt showed only ~15% color fading[36] after one year (compared to ~45% for an untreated control). It maintained superhydrophobicity throughout (Supplementary Fig. 15c). Even after extensive abrasion and washing, the treated fabrics maintain very low sliding angles (<5°) (Supplementary Fig. 16, SEM images in Supplementary Table 3). These results demonstrate that the MARS technique endows fabrics with exceptional durability and wear resistance, enabling them to retain superhydrophobicity under a variety of mechanical stresses and environmental conditions, making them suitable for practical, long-term use in garments and outdoor applications.

Robust Superhydrophobicity under Harsh Conditions

Superhydrophobic textiles are also sought for preventing scalding injuries from hot liquids soaking into clothing, yet most existing water-repellent garments are ineffective against very hot fluids[42,43]. MARS-modified textiles demonstrated excellent repellency even for hot water. When 85°C water droplets (Weber number ~15) impacted the fabric, they still bounced off cleanly (Fig. 4a). Tests with a continuous hot water jet (85°C, ~0.5 $\mathrm{m \cdot s^{-1}}$ flow) and a burst of hot coffee steam (100°C, 9 bar pressure, 150 mL) showed consistent water-repellent performance (Fig. 4b, c; Supplementary Movie 5), far more effective than a comparable fluorinated treatment[44]. Even under extreme alternating thermal conditions, MARS-treated fabrics withstood sequential jetting with boiling water (95°C, 250 mL, 30 s), liquid nitrogen (-196°C, 250 mL, 200 s), and boiling water again (95°C, 250 mL, 30 s), yet still retained superhydrophobicity at the end (Fig. 4d, Supplementary Fig. 17, Supplementary Movie 5).

Another challenge for hot liquid repellency in textiles is resistance to steam. After exposure to 160°C steam, MARS textiles immediately shed water droplets, whereas perfluorosilane-treated controls became wetted by the steam (Fig. 4e, f, Supplementary Movie 5). Low-field NMR measurements revealed that steam-exposed PFAS-treated samples retained free-water signals lasting ~2000 ms. In contrast, MARS fabrics showed only weak, long T_2 signals corresponding to semi-free water, evidencing that the covalent silica network effectively blocks vapor condensation (Supplementary Fig. 6f). PFAS-free MARS superhydrophobic coatings thus provide more reliable hot-water protection. Furthermore, the high-density covalent bonding in the MARS coating ensures stability under steam. When we sealed a bottle of boiling water with a spray-coated superhydrophobic fabric (Capstone-FS), steam became trapped and condensed within the fabric pores[29,45], destroying its breathability. By comparison, the MARS-modified fabric allowed steam to pass through (evidenced by condensed water appearing on a glass slide above the textile), and water droplets impacting the fabric opening simply rolled off (Supplementary Fig. 18).

The MARS modification collectively enhances long-term water repellency, wear resistance, and steam resistance, addressing three key challenges faced by superhydrophobic textiles. The high-density silica network in MARS confers superhydrophobicity. It traps a stable air layer at the textile-water interface, which is vital for maintaining breathability and reducing drag in water[17,46], similar to the water-shedding strategy of penguin feathers[20]. Air permeability tests[47] confirmed that the treated fabric allows rapid airflow and maintains breathability over extended periods (≥13.5 hours, Supplementary Fig. 19, Supplementary Movie 6). In dynamic underwater tests, MARS-treated leggings effectively repelled water during repeated kicking motions in a swimming pool (Fig. 4g). The fabric maintained a stable plastron air cushion[48], as evidenced by strong light reflection, even at a flow velocity of 2.0 $m \cdot s^{-1}$ in a water tunnel (Fig. 4h, Supplementary Fig. 20, Supplementary Movie 7). Moreover, MARS textiles exhibited a ~40% drag reduction compared to untreated fabrics over 1 hour at a flow rate of 0.5 $m \cdot s^{-1}$ (Fig. 4i).

The coating's safety is our final concern. We conducted cytotoxicity and cell proliferation assays (5-day CCK-8 test using NIH 3T3 fibroblasts) to evaluate the MARS coating's safety (Supplementary Fig. 21). The results showed no significant difference in cell viability or growth between the MARS-coated fabric and an untreated control. In contrast, a fabric treated with a PFAS-based water repellent (Capstone-FS, containing PFOS) exhibited only about half the viable cell count of the other two groups by day 5. MARS is analogous to silica (sand/glass) combined with long-chain paraffin wax, the materials of which are widely regarded as inert, non-toxic, and biocompatible.

Discussion

Silane-based cross-linked networks have been explored on other substrates, such as paper[49-51], metal electrodes[52], and textiles[53,54]. However, those studies primarily demonstrated superhydrophobicity without thoroughly examining wear resistance in practical conditions. Our MARS approach, with a well-defined core-shell mushroom-like aggregate structure, yields shells covalently bonded to the fibers, thereby providing high mechanical strength and strong adhesion for other applications. By achieving superhydrophobicity at the single-fiber level, we enable the creation of woven and knitted textiles that strike a balance between functionality, comfort, and sustainability[13]. Our approach is particularly suitable for outdoor, protective, and high-performance applications, and also paves the way for future innovations in electronic fabrics[55], display textiles[56], and wearable healthcare monitors[57,58].

Methods

Superhydrophobic Fabric Preparation

Materials and Reagents Natural fibers (cotton, wool, and linen) and synthetic fibers (nylon and polyester) were obtained from Haixu Fiber Products and kindly provided by ANTA Sport. LINING kindly supplied the Jacquard-woven shoe upper. Reagents for superhydrophobic treatment include tetrachlorosilane (TCS), octadecyltrichlorosilane (OTS), and anhydrous petroleum ether (anhydrous grade), which were purchased from Alfa Aesar. Carbon nanofibers (100 nm diameter, 20-200 μm length) served as substrates for TEM imaging of the amorphous SiO_2 network (Supplementary Fig. 5a), which were purchased from Sigma-Aldrich.

The superhydrophobic coating process is performed using a homemade device in a fuming hood. Twisted yarns (150D, 36F) were continuously drawn through a petroleum ether solution containing 4 wt% TCS and 2 wt% OTS at a linear speed of 0.25 $m \cdot s^{-1}$. The take-up speed of the winding machine (HR3688, Hangzhou Hengji Machine Co. Ltd.) controlled the reaction time in the solution, and silane concentrations were optimized to yield a uniform silica shell coating (Supplementary Fig. 1-3). Then, the fibers were dried in humid air (relative humidity, RH 95%) for several seconds to allow solvent evaporation and silane hydrolysis to occur.

Coated yarns were then processed into textiles, with weaving and machine knitting carried out by Xiexin Worsted Spinning Weaving and Dyeing Co., Ltd. in Wuxi, China. To produce patterned superhydrophobic motifs, MARS-treated yarns were embroidered onto untreated fabric substrates using standard embroidery machines (Innovis brother-NV180, Japan). The T-shirt shown in Supplementary Movie 3 was knitted using cotton yarns that were pre-treated *via* the continuous MARS process by Sinotex SNT-803S (Hi-Tech Group Corporation, China). The detail weaving process was shown in Supplementary Movie 8.

For comparison, identical fabrics were spray-coated with (1) hydrophobic nanobeads (Ultra-Ever Dry, Ultratech International) and (2) a 1:1 mixture of Capstone ST-200 (DuPont) and fused silica (Aerosil R202, Evonik).

Characterization of MARS Treated Fabric

Characterization and Measurements Optical images were captured with a digital camera (Nikon D750, Japan). Surface morphology and stereomicroscopic images of abraded areas were obtained using a stereomicroscope (Olympus DSX1000, Japan). Scanning electron microscopy (SEM) was performed using a field-emission scanning electron microscope (Hitachi SU8010, Japan) at an accelerating voltage of 5 kV. The samples were sputter-coated with a thin platinum layer (Leica EM ACE600, Germany). Transmission electron microscopy (TEM) images were acquired on a FEI Tecnai G2 F20 (USA) at 200 kV, using carbon nanofiber substrates to visualize the amorphous SiO_2 network. High-resolution microcomputed tomography (micro-CT; Bruker SkyScan 1272, USA) was used to visualize the water-solids interface within droplets on the superhydrophobic textiles. A droplet seated on the textiles was mounted in a custom holder, and dynamic scanning commenced before the liquid reached the notched region. Projections were recorded at 4K resolution (6.0 μm voxel size) and optimized at an X-ray energy of 30 keV. X-ray photoelectron spectroscopy (ThermoFisher ESCALab 250Xi, USA) was used to determine the elemental composition of the treated fabrics. Low-field nuclear magnetic resonance (LF-NMR; Niumag VTMR20-010V-I, China) was used to characterize the water-binding properties in treated fibers. Scrub resistance was test by QFS-scrub resistance tester (Shanghai Meiyu Technology Instrument BH14J, China). Figures 2a, b, d, e, f; 3a, b, g, h, i; Supplementary Figures 1a, 8a, b, and 20a were created using PS software.

The color fastness of the MARS-modified fabrics was evaluated using a colorimeter (CHNSpec DS-220, China) to calculate color differences before and after modification. We utilized the CIE $L^*a^*b^*$ color space model, which enables the calculation of color differences based on lightness (L^*), red-green (a^*), and yellow-blue (b^*) components. The color difference, $\Delta E^*=\sqrt{(L_1-L_2)^2+(a_1-a_2)^2+(b_1-b_2)^2}$, where L_1, a_1, and b_1 are the color coordinates before MARS modification, and L_2, a_2, and b_2 are the coordinates after modification. The whiteness of the MARS-modified fabrics was evaluated by a whiteness meter (Qiwei WSB-1, China).

Water Repellency and Contact Angle Measurement

Static water contact angles were measured on fabric surfaces using a KRÜSS DSA 25S goniometer (Germany) with 2.0 μL droplets and a KRÜSS DSA 30M drop-shape analyzer equipped with a 20× microscope objective and piezoelectric micro-dosing head for 20–200 pL droplets. Static water contact angles were measured with a contact angle goniometer across droplet diameters from 10 μm to 2 mm to evaluate hydrophobicity over a range of scales. Each fabric sample was tested at five distinct locations; the reported values represent the mean ± standard deviation.

Liquid jets impact test

High-speed imaging of droplet and sand impacts was performed using a PHOTRON FASTCAM Nova S20 (Japan) at a frame rate of 1,000 fps. Droplets (D = 1.0 mm) were released from a needle positioned 10.0 mm above the fabric to achieve an impact velocity of 0.45 $m\cdot s^{-1}$. Side-view dynamics were captured at 10,000 frames per second (fps) with backlighting to determine impact velocity and contact time. A Harvard Apparatus micro-injection gear pump (USA) controlled liquid flow rates. When testing hot water (25°C vs. 85°C), surface tension γ decreases from 72 mN/m to 62 mN/m. Continuous liquid-jet impacts were recorded with a PHOTRON FASTCAM Nova S20 and a macro lens at 2,000 fps. Infrared thermography was conducted with a FLIR A600 camera (USA).

Wash test

MARS-treated, Capstone-FS-treated, and Ultra-Ever Dry-treated fabric samples (20 × 20 cm) were laundered in a standard home washing machine (high-efficiency front-loading type). After each wash cycle, water repellency was evaluated using the AATCC 22-2017 spray test standard. In this test, 250 mL of distilled water is poured through a funnel with 19 holes (each ~0.86 mm diameter) from 150 mm above the fabric, which is held at a 45° angle. The fabric's wetting is assessed by the amount of water sticking to the surface, the number of wetted spots, and the area wetted. Each fabric was tested in triplicate. Detailed laundering conditions followed AATCC LP1-2021 for machine washing, using AATCC standard reference detergent (AATCC M1-2017e). Key wash parameters included: a 15 ± 4 L water fill, 1.8 ± 0.1 kg load, 50 ± 1 mL detergent, agitation at 45 ± 10 rpm for 11 ± 1 minutes, 2 rinse cycles, final spin at 1300 ± 150 rpm for 12–18 minutes, and wash water temperature 25 ± 3 °C (see Supplementary Table 5 for the full set of parameters).

Abrasion Resistance (Martindale, Taber test)

Abrasion resistance was evaluated using Martindale and Taber testers (Darong Textile Instrument, China). Martindale test was performed following ASTM D4966. Fabric samples were secured to the Martindale head and abraded against standard wool felt under a pressure of 9 kPa in a Lissajous pattern for 80,000 cycles. The Taber test was performed in accordance with ASTM D4060. Circular fabric specimens (100 mm diameter) were mounted on a rotating platform, and two counter-rotating CS-10 grinding wheels (each with a 250 g load) rubbed the sample for up to 20,000 cycles, generating both inward and outward wear tracks. Abrasion depth was evaluated by observing changes in thickness and appearance by a stereo microscope (Olympus DSX1000, Japan). After every 2,000 cycles, static contact angles were re-measured to confirm sustained superhydrophobicity.

Peel Adhesion Test

The adhesion of the MARS layer was quantified using 3M peel tests (ASTM D3330-2018). A 3M bonding tape was applied with a 4 kg roller (two passes), left for 90 s, and then peeled at 90° using a custom fixture conforming to ASTM D6862 (ASTM D6862-2021 Standard test method for 90 degree peel resistance of adhesives) on a Mark-10 ESM303 force platform (USA). Each cycle used fresh tape. After peeling off, the local water contact angle was measured using a ~2 μL droplet.

Falling Sand Impact

Abrasion resistance under falling-sand impact was assessed per ASTM D968-2025. Silica sand (400-700 μm) was released from 91.4 cm above the fabric, striking at a 45° angle with an impact velocity of ~ 4.2 $m \cdot s^{-1}$. High-speed imaging of sand impacts was performed using a PHOTRON FASTCAM Nova S20 (Japan) at a frame rate of 2,000 fps. Post-impact, superhydrophobicity and surface integrity were evaluated using contact angle measurements and SEM imaging.

Fabric touch test

The fabric handling properties were quantified using the fabric touch tester (Darong Textile Instrument DR555FT, China). The device evaluated the four different dimensions of the untreated, MARS-treated, and Capstone-FS-treated fabric physical properties: the compression, thermal, surface, and bending properties (including pulling, pressing, pinching, kneading, and rubbing). The fabric samples were cut into an L-shaped configuration (310 × 310 mm) with 200 mm arms.

The central square region of each specimen was subjected to a downward pulling force, inducing horizontal displacement in the two arm sections. Compression properties were measured at the central area of the sample, while bending and surface characteristics were evaluated along the arm sections. To ensure measurement efficiency, the bending and surface modules were designed for duplicate testing, allowing bidirectional assessment of each sample in a single test cycle.

Environmental Durability Testing

Hot Coffee Resistance Heated coffee (> 80°C), extracted from a Starbucks Verdana Blend Americano capsule and pressurized on Dolce Gusto machines (De'Longhi, Italy), was directly applied to MARS- and Capstone-FS-treated fabrics for 30 s (150 mL). The treated fabric samples are placed at an angle of 60°. Surface wetting state during coffee impact was monitored by infrared thermography. The impact event was recorded at 100 frames per second (fps) using a FLIR A600 camera (USA) fitted with a macro lens.

Thermal Stability Thermal cycling was performed by alternately exposing samples to boiling water (100 °C; 300 mL dispensed over 30 s via a Xiaomi Smart Water Dispenser, China) and liquid nitrogen (-196 °C; ~300 mL poured over 30 s). After each hot-cold or cold-hot cycle, static contact angles and droplet rebound behavior were re-evaluated to assess the retention of superhydrophobicity.

High-Temperature Steam Resistance Treated fabrics were placed in a splint-type steam iron set to 160°C for 10 s of direct steam exposure. After steaming, colored water was jetted onto the fabric surface, and surface wettability was recorded. Optical videos were captured at 50 frames per second (fps) using a Nikon D750 camera (Japan), while infrared thermal imaging was recorded at 100 frames per second (fps) with the FLIR A600 (USA).

Stable Air Cushion at the Fabric-Water Interface The experiment was conducted in a swimming pool. The MARS-treated legging was fitted onto a prosthetic limb, which was then submerged underwater to a depth of 5 cm by a robotic arm (R630, Beijing SDCQ Electrical Technology Co., Ltd., China) at a frequency of 10 cycles per minutes. An underwater camera (DJI Action2, China) was used to record the fabric-water interface.

Water Tunnel Experiment The drag reduction capability of the superhydrophobic fabrics was tested in a circulating water tunnel at a flow velocity of 0.5 to 2.0 m·s^{-1}. The fabric samples were fixed in the flow stream, and the drag force was measured using a force transducer. Drag reduction efficiency was calculated as (F_{control} - F_{test})/F_{control} × 100, where F_{control} is the drag force on a control (untreated) fabric, and F_{test} is the drag force on the superhydrophobic fabric.

Data Availability

All relevant data supporting the key findings of this study are available within the article and its Supplementary Information or from the corresponding author upon reasonable request. Source data are provided with this paper.

References

1. Li, L. et al. Challenges and strategies for commercialization and widespread practical applications of superhydrophobic surfaces. *Sci. Adv.* **9**, eadj1554 (2023).
2. Pan, S. et al. Coatings super-repellent to ultralow surface tension liquids. *Nat. Mater.* **17**, 1040-1047 (2018).
3. Lu, Y. et al. Robust self-cleaning surfaces that function when exposed to either air or oil. *Science* **347**, 1132-1135 (2015).
4. Tian, X., Verho, T. & Ras, R. H. A. Moving superhydrophobic surfaces toward real-world applications. *Science* **352**, 142-143 (2016).
5. Geyer, F. et al. When and how self-cleaning of superhydrophobic surfaces works. *Sci. Adv.* **6**, eaaw9727 (2020).
6. Artus, G. R. J. et al. Silicone nanofilaments and their application as superhydrophobic coatings. *Adv. Mater.* **18**, 2758-2762 (2006).
7. Zimmermann, J., Reifler, F. A., Fortunato, G., Gerhardt, L. C. & Seeger, S. A simple, one-step approach to durable and robust superhydrophobic textiles. *Adv. Funct. Mater.* **18**, 3662-3669 (2008).
8. Tian, T. et al. Large-area waterproof and durable perovskite luminescent textiles. *Nat. Commun.* **14**, 234 (2023).
9. Deng, X., Mammen, L., Butt, H. J. & Vollmer, D. Candle soot as a template for a transparent robust superamphiphobic coating. *Science* **335**, 67-70 (2012).
10. Verho, T. et al. Mechanically durable superhydrophobic surfaces. *Adv. Mater.* **23**, 673-678 (2010).
11. Huang, S., Li, J., Chen, L. & Tian, X. Suppressing the universal occurrence of microscopic liquid residues on super-liquid-repellent surfaces. *J. Phys. Chem. Lett.* **12**, 3577-3585 (2021).
12. Lim, X. Could the world go PFAS-free? Proposal to ban ‘forever chemicals’ fuels debate. *Nature* **620**, 24–27 (2023).
13. Evich, M. G. et al. Per- and polyfluoroalkyl substances in the environment. *Science* **375**, eabg9065 (2022).
14. Fang, J. et al. Treatment of per- and polyfluoroalkyl substances (PFAS): A review of transformation technologies and mechanisms. *J. Environ. Chem. Eng.* **12**, 111833 (2024).
15. Wang, D. et al. Design of robust superhydrophobic surfaces. *Nature* **582**, 55-59 (2020).
16. Barthlott, W. & Neinhuis, C. Purity of the sacred lotus, or escape from contamination in biological surfaces. *Planta* **202**, 1-8 (1997).
17. Feng, L. et al. Super-hydrophobic surfaces: From natural to artificial. *Adv. Mater.* **14**, 1857-1860 (2002).
18. Barthlott, W. et al. The *Salvinia* paradox: superhydrophobic surfaces with hydrophilic pins for air retention under water. *Adv. Mater.* **22**, 2325-2328 (2010).
19. Wisdom, K. M. Self-cleaning of superhydrophobic surfaces by self-propelled jumping condensate. *Proc. Natl. Acad. Sci. USA* **110**, 7992-7997 (2013).
20. Wood, M. J., Brock, G. & Kietzig, A. M. The penguin feather as inspiration for anti-icing surfaces. *Cold Reg. Sci. Technol.* **213**, 103903 (2023).
21. Helbig, R., Nickerl, J., Neinhuis, C. & Werner, C. Smart skin patterns protect springtails. *Plos One* **6**, e25105 (2011).
22. Friedrichs, J. et al. Entropic repulsion of cholesterol-containing layers counteracts bioadhesion. *Nature* **618**, 733-739 (2023).
23. Hensel, R., Neinhuis, C. & Werner, C. The springtail cuticle as a blueprint for omniphobic surfaces. *Chem. Soc. Rev.* **45**, 323-341 (2016).
24. Tuteja, A. et al. Designing superoleophobic surfaces. *Science* **318**, 1618-1622 (2007).

25. Liu, T. L. & Kim, C. J. C. Turning a surface superrepellent even to completely wetting liquids. *Science* **346**, 1096-1100 (2014).
26. Hyde, J. F. Chemical background of silicones: The siloxane linkage as a structure-building device gives variety and versatility to the silicones. *Science* **147**, 829-836 (1965).
27. Vũ, N. Đ. et al. Gallium-catalyzed recycling of silicone waste with boron trichloride to yield key chlorosilanes. *Science* **388**, 392-400 (2025).
28. Fang, G. et al. Stepwise mechanism and H_2O-assisted hydrolysis in atomic layer deposition of SiO_2 without a catalyst. *Nanoscale Res. Lett.* **10**, 1-7 (2015).
29. Quéré, D. Fluid coating on a fiber. *Annu. Rev. Fluid Mech.* **31**, 347-384 (1999).
30. Ignatov, S. K. et al. Theoretical study of the reaction mechanism and role of water clusters in the gas-phase hydrolysis of $SiCl_4$. *J. Phys. Chem. A* **107**, 8705-8713 (2003).
31. Song, Y., Nair, R. P., Zou, M. & Wang, Y. Superhydrophobic surfaces produced by applying a self-assembled monolayer to silicon micro/nano-textured surfaces. *Nano Res.* **2**, 143-150 (2010).
32. Moronuki, N., Takada, T. & Schotten, A. Dynamic contact angle measurement on a microscopic area and application to wettability characterization of a single fiber. *Langmuir* **38**, 72-78 (2021).
33. Lam, C. W. E. et al. Condensate droplet roaming on nanostructured superhydrophobic surfaces. *Nat. Commun.* **16**, 1167 (2025).
34. Cassie, A. B. D. & Baxter, S. Large contact angles of plant and animal surfaces. *Nature* **155**, 21-22 (1945).
35. Eder, M., Amini, S. & Fratzl, P. Biological composites—complex structures for functional diversity. *Science* **362**, 543-547 (2018).
36. Kotsidi, M. et al. Preventing colour fading in artworks with graphene veils. *Nat. Nanotechnol.* **16**, 1004-1010 (2021).
37. Milionis, A., Loth, E. & Bayer, I. S. Recent advances in the mechanical durability of superhydrophobic materials. *Adv. Colloid Interface Sci.* **229**, 57-79 (2016).
38. British Standards Institution, 1993. BS/EN/ISO 29865:1993 Determination of water repellency of fabrics by the Bundesmann rain-shower test. British Standards Institution, London.
39. Chu, Z. & Seeger, S. Superamphiphobic surfaces. *Chem. Soc. Rev.* **43**, 2784-2798 (2014).
40. Wong, W. S. Y. et al. Design of fluoro-free surfaces super-repellent to low-surface-tension liquids. *Adv. Mater.* **35**, 202300306 (2023).
41. Cavagna, G. A. & Franzetti, P. The determinants of the step frequency in walking in humans. *J. Physiol.* **373**, 235-242 (1986).
42. Katcher, M. L. Prevention of tap water scald burns: Evaluation of a multi-media injury control program. *Am. J. Public Health* **77**, 1195-1197 (1987).
43. Liu, Y., Chen, X. & Xin, J. H. Can superhydrophobic surfaces repel hot water? *J. Mater. Chem.* **19**, 5602-5611 (2009).
44. Li, B. & Zhang, J. Durable and self-healing superamphiphobic coatings repellent even to hot liquids. *Chem. Commun.* **52**, 2744-2747 (2016).
45. Duprat, C. Moisture in textiles. *Annu. Rev. Fluid Mech.* **54**, 443-467 (2022).
46. Hu, H. et al. Significant and stable drag reduction with air rings confined by alternated superhydrophobic and hydrophilic strips. *Sci. Adv.* **3**, e1603288 (2017).
47. de Maleprade, H., Clanet, C. & Quéré, D. Spreading of bubbles after contacting the lower side of an aerophilic slide immersed in water. *Phys. Rev. Lett.* **117**, 094501-094505 (2016).
48. Mehanna, Y. A. et al. The challenges, achievements and applications of submersible superhydrophobic materials. *Chem. Soc. Rev.* **50**, 6569-6612 (2021).
49. Liu, S. et al. Printable and versatile superhydrophobic paper via a scalable nonsolvent armor strategy. *ACS Nano* **16**, 9442–9451 (2022).

50. Liu, X. et al. Design and synthesis of a robust and multifunctional superhydrophobic coating with a three-dimensional network structure on a paper-based material. *ACS Appl. Mater. Interfaces* **16**, 37111–37121 (2024).

51. Zhang, J. & Seeger, S. Superoleophobic coatings with ultralow sliding angles based on silicone nanofilaments. *Angew. Chem. Int. Ed.* **50**, 6652–6656 (2011).

52. Wang, Y. et al. Lithium metal electrode with increased air stability and robust solid electrolyte interphase realized by silane coupling agent modification. *Adv. Mater.* **33**, 2008133 (2021).

53. Yu, M. et al. Positive effect of polymeric silane-based water repellent agents on the durability of superhydrophobic fabrics. *Appl. Surf. Sci.* **450**, 492–501 (2018).

54. Phelan, M., Goff, C., Ward, M. & Thai Trung King, M. *Superhydrophobic coatings for the treatment of textiles.* U.S. Patent US20200299541A1 (2020).

55. Zhang, K. et al. Design and fabrication of wearable electronic textiles using twisted fiber-based threads. *Nat. Protoc.* **19**, 557-1589 (2024).

56. Shi, X. et al. Large-area display textiles integrated with functional systems. *Nature* **591**, 240-245 (2021).

57. Heng, W. et al. A smart mask for exhaled breath condensate harvesting and analysis. *Science* **385**, 954-961 (2024).

58. Zhang, B. et al. A three-dimensional liquid diode for soft, integrated permeable electronics. *Nature* **628**, 84-92, (2024).

Acknowledgments

We thank Dr. Shihui Zhu (TIPC) for initiating the request that our team prepare non-PFAS superhydrophobic cloth samples for the Science and Technology Festival at the Chinese Academy of Sciences since 2020. The MARS coat has been shown to more than 10^4 sWe are deeply appreciative of Z. Hong and T. Cai from China Strait Talent Market and the Shishi government for their generous assistance throughout the research, especially in the textile weaving and cloth production processes. We are grateful to L. Tian for technical assistance with Environmental SEM; Dr. W. Zhang of LINING Co. Ltd. for providing yarns and shoe vamps; and Dr. Z. Xiong, Y. Liu, and H. Zhi of ANTA Sports Co. Ltd. for supplying yarns and fabrics. We also thank Prof. J. Su (Jiangnan University) for support with knitting, and Dr. S. Hou and Dr. J. Zhang (KRUSS, China) for conducting the fiber contact-angle measurements. We acknowledge Darong Textile Instrument Co., Ltd. for providing standard textile testing equipment, Dr. J. Xiang for technical support, and Dr. H. Ding (Suzhou Niumag Analytical Instrument) for assistance with low-field NMR measurements. We express our sincere gratitude to Dr. T. Cai, Dr. F. Zheng, and Engineer Cai of the China Textile Academy Institute for their expert guidance during performance testing. We further express our sincere gratitude to Chairman Y. Chen from Wujiang Hanta Textile Finishing Co., Ltd., for the production of the final products. We thank the 17 instructors of Group 3 of the 9th CAS Young and Middle-Aged Talent Training Program for testing the textile T-shirts and providing valuable feedback throughout September 2025. We acknowledge project funding from the National Natural Science Foundation (22122508 and 52173293 to ZD) and the Young Elite Scientists Sponsorship Program of the China Association for Science and Technology (ZD).

Author contributions

ZD conceived and designed the project, supervising all aspects. LZ and DH were responsible for material preparation and testing characterization assisted by KZ, SL, ZZ and LW. LZ, JM and DH analyzed the experimental data. ZL, DH, ZD wrote the original manuscript. LW and ZD supervised the work, offered project support, and revised the manuscript. All authors participated in the discussion.

Competing interests

The MARS superhydrophobic fabric preparation method is covered by three pending CNIPA patents: CN 202610186197.5 (2026.02.09), CN 202610194657.9 (2026.02.11) and CN 202610208747.9 (2026.02.13). Applicants: Beijing Institute of Future Science and Technology on Bioinspired Interface. Inventors Zhichao Dong, Zhuoxing Liu and Dezhao Hao are also paper authors. Authors declare that they have no competing interests.

Figure legends

Fig. 1 | Biomimetic inspiration and MARS-modification process. a, Springtails thrive in wet environments and jump on water surfaces using superhydrophobic skin. **b**, SEM image of springtail cuticle, showing hierarchical nano-ridges and mushroom-shaped structures. Scheme demonstrating the mushroom-shaped structures that prevent water adhesion and maintain air pockets. **c**, Schematic illustration of the molecular-assembled robust-superhydrophobic shells (MARS) process on twisted yarns. **d**, SEM image of a yarn after treatment, displaying hierarchical silica shell structures with mushroom-like aggregates. **e**, Water droplets on MARS-modified yarn maintain contact angles of ~160°. **f**, Water condensation on MARS-modified yarns slid off the surface upon reaching a diameter of 2 µm. **g**, The MARS-modified fibers were woven into superhydrophobic textiles, and the contact angle of water droplets is 154.7°. **h**, The MARS-modified fibers were knitted into superhydrophobic textiles, retaining high apparent contact angles of 156.1°. Micro-CT imaging demonstrates the internal structure and water droplet behavior on the fabric surface, providing a clear view of the material's superhydrophobic properties. **i**, Embroidery process using MARS-treated yarns on white handkerchiefs. The embroidery machine stitches the yarn into the fabric, and despite friction between the needle and the yarn, the superhydrophobicity of yarns remains intact. Photo credit of embroidery in (i): Z.L., Chinese Academy of Sciences.

Fig. 2 | Superhydrophobic performance of MARS-modified fabric. a, Superhydrophobic performance of MARS-modified white T-shirt, black leggings, and white vamp. **b**, Water repellency spray test (AATCC 22) demonstrated that MARS-modified fabric retains its superhydrophobicity after being sprayed 100 times. **c**, Dynamic impact test showing droplet rebound behavior for cold (25°C) water droplets. **d**, The raindrop impact simulation setup demonstrates a single-point impact threshold, confirming the durability of the 10^4 impact times. **e**, A rotation setup simulation of high-speed raindrop impacts ($11.6\ \mathrm{m \cdot s^{-1}}$) confirms durability under harsh conditions. **f**, Bundesmann rain-shower test results confirm low water absorption rates and penetration resistance. Data in (d, f) are shown as mean ± SD and the error bar represents SD (n = 3). Source data for (d and f) are provided as a Source Data file. Photo credit of Superhydrophobic performance in (a): Z.L., Chinese Academy of Sciences.

Fig. 3 | Durability of MARS-treated fabrics under mechanical stress. a, **b**, Contact angle variations follow repeated abrasion cycles using the Martindale (**a**) and Taber abrasion (**b**) methods. **c**, Contact angle variations of the treated fabrics during sand abrasion cycles. **d**, Radar chart for comparing primary sensory indices from the fabric touch tester results of untreated, MARS-treated, and Capstone-FS-treated fabrics. The physical indicators include fabric compression, bending, surface roughness, and surface friction. Detailed indicators are shown in Supplementary Table 2. **e**, Running induces wear on T-shirts. **f**, Shoulder-strap friction wear test of treated T-shirts under backpack mesh pressure for 600,000 cycles. **g**, Contact angle variations of the knitted fabrics during stretch-release cycles. **h**, Contact angle variations during the scrub resistance test. **i**, Contact angle and peeling force variations with tape peeling-off cycles. **j**, Treadmill continuous walking frictional wear test for 15,000 steps at 51.3 kPa of pressure. **k**, The variation of the contact angle difference between the Capstone-FS and MARS-modified fabrics after walking 15,000 steps. Data in (a-c, f-i and k) are shown as mean ± SD and the error bar represents SD (n = 5).

Source data for (a-c, f-i and k) are provided as a Source Data file. Photo credit of sand abrasion performance in (c): Z.L., Chinese Academy of Sciences.

Fig. 4 | Superhydrophobic performance under environmental and thermal stress conditions. a, Hot water droplets bounce up to three times. **b**, Resistance to hot water jets on MARS-modified fabrics. **c**, The MARS-modified fabrics repel hot coffee (100°C, 9 bar pressure, 150 mL), confirming consistent water-repellent performance. **d**, Durability under alternating extreme temperature cycles of liquid nitrogen (-196°C) and hot water (95°C) exhibits no loss of repellency. **e**, Experimental setup of high-temperature steam ironing (160°C). **f**, MARS-modified fabrics can withstand high-temperature steam (160°C) and repel water droplets soon after steam ironing. **g**, Stability of the air layer at the fabric-water interface of the MARS-modified legging. **h**, Entrapped air layer, visualized under water flow velocities of 2.0 $m \cdot s^{-1}$, confirmed by light reflection. **i**, Drag reduction of MARS-modified fabrics. Data in (i) is shown as mean ± SD and the error bar represents SD (n = 3). Source data for (i) are provided as a Source Data file. Photo credit of sand abrasion performance in (e-f): Z.L., Chinese Academy of Sciences.

Additional information

Supplementary information The online version contains supplementary material available for this paper.

Correspondence and requests for materials should be addressed to Zhichao Dong.

Peer review information includes the names of reviewers who agree to be cited and is completed by *Nature Communications* staff during proofing.

Reprints and permissions information is available at http://www.nature.com/reprints.

Editor’s summary:

Developing durable, water-repellent textiles without using harmful fluorinated chemicals is challenging. Here, authors use a one-step molecular assembly to covalently bond superhydrophobic silica shells directly onto fibers, resulting in high wear resistance and breathability.

Peer review information: *Nature Communications* thanks Nusret Celik and the other anonymous reviewer(s) for their contribution to the peer review of this work. A peer review file is available.

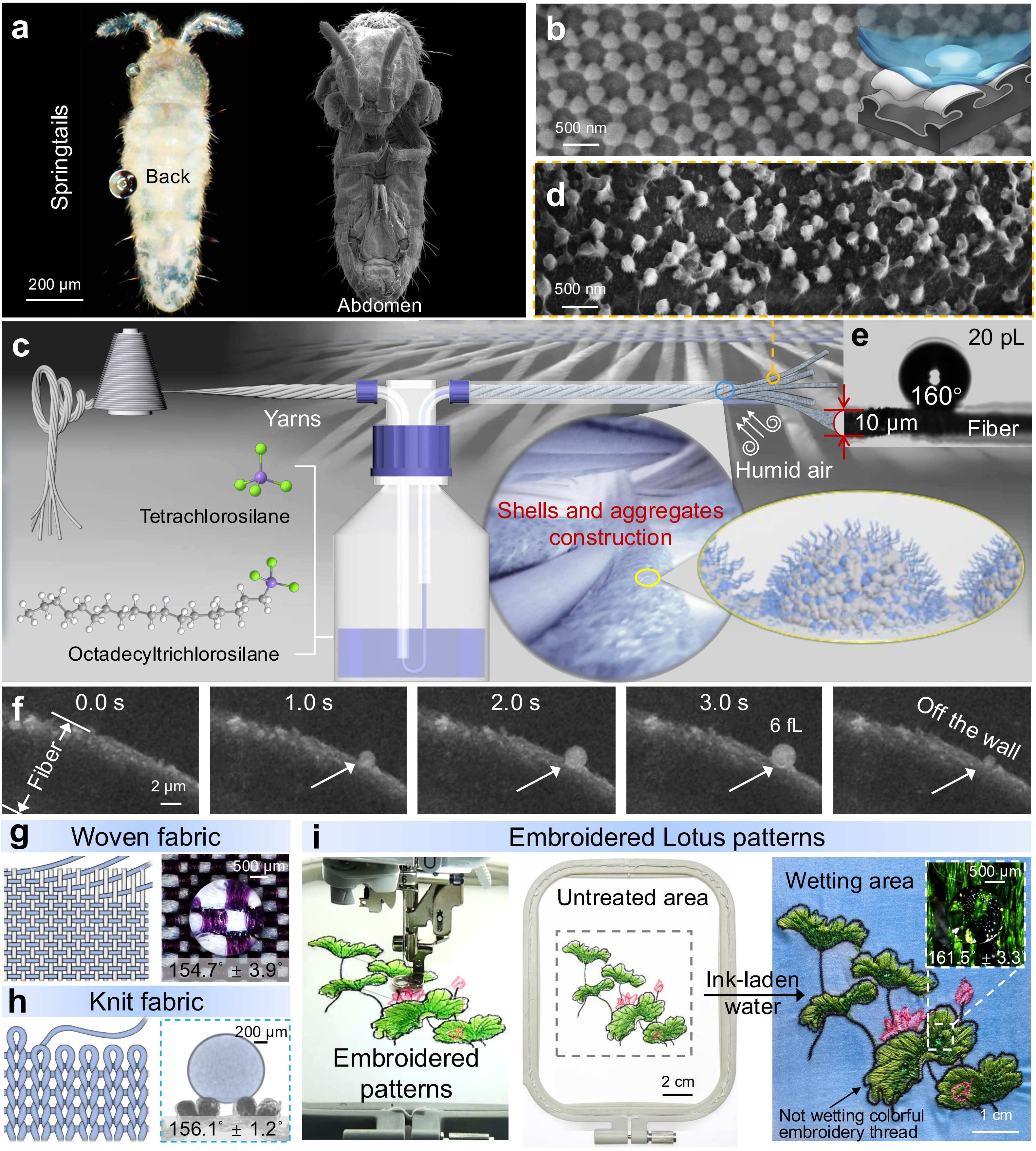
a
Springtails
Back
200 µm
Abdomen
b
500 nm
d
500 nm
c
Yarns
Tetrachlorosilane
Octadecyltrichlorosilane
Shells and aggregates construction
Humid air
e
20 pL
160°
10 µm
Fiber
f
0.0 s
Fiber
2 µm
1.0 s
2.0 s
3.0 s
6 fL
Off the wall
g
Woven fabric
500 µm
154.7° ± 3.9°
h
Knit fabric
200 µm
156.1° ± 1.2°
i
Embroidered Lotus patterns
Embroidered patterns
Untreated area
2 cm
Ink-laden water
Wetting area
500 µm
161.5° ± 3.3°
Not wetting colorful embroidery thread
1 cm

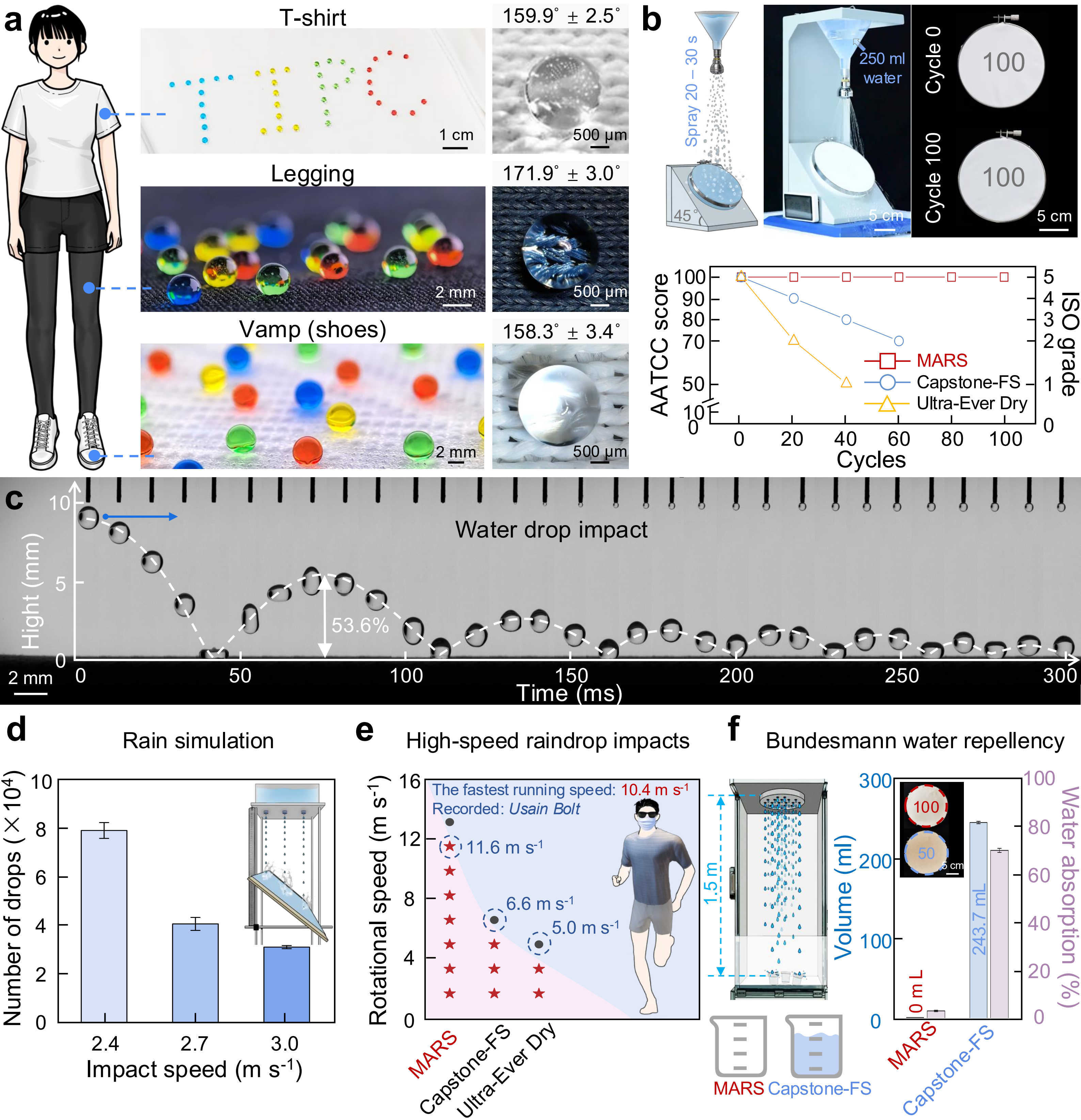
a
T-shirt
159.9° ± 2.5°
1 cm
500 μm
Legging
171.9° ± 3.0°
2 mm
500 μm
Vamp (shoes)
158.3° ± 3.4°
2 mm
500 μm
b
Spray 20 – 30 s
45°
250 ml water
5 cm
Cycle 0
100
Cycle 100
100
5 cm
AATCC score
100
90
80
70
50
10
0
ISO grade
5
4
3
2
1
0
Cycles
0
20
40
60
80
100
MARS
Capstone-FS
Ultra-Ever Dry
c
Water drop impact
Hight (mm)
10
5
0
53.6%
2 mm
Time (ms)
0
50
100
150
200
250
300
d
Rain simulation
Number of drops (×10⁴)
10
8
6
4
2
0
2.4
2.7
3.0
Impact speed (m s⁻¹)
e
High-speed raindrop impacts
The fastest running speed: 10.4 m s⁻¹
Recorded: Usain Bolt
Rotational speed (m s⁻¹)
16
12
8
4
0
11.6 m s⁻¹
6.6 m s⁻¹
5.0 m s⁻¹
MARS
Capstone-FS
Ultra-Ever Dry
f
Bundesmann water repellency
1.5 m
MARS
Capstone-FS
Volume (ml)
300
200
100
0
Water absorption (%)
100
80
60
40
20
0
100
50
5 cm
0 mL
243.7 mL
MARS
Capstone-FS

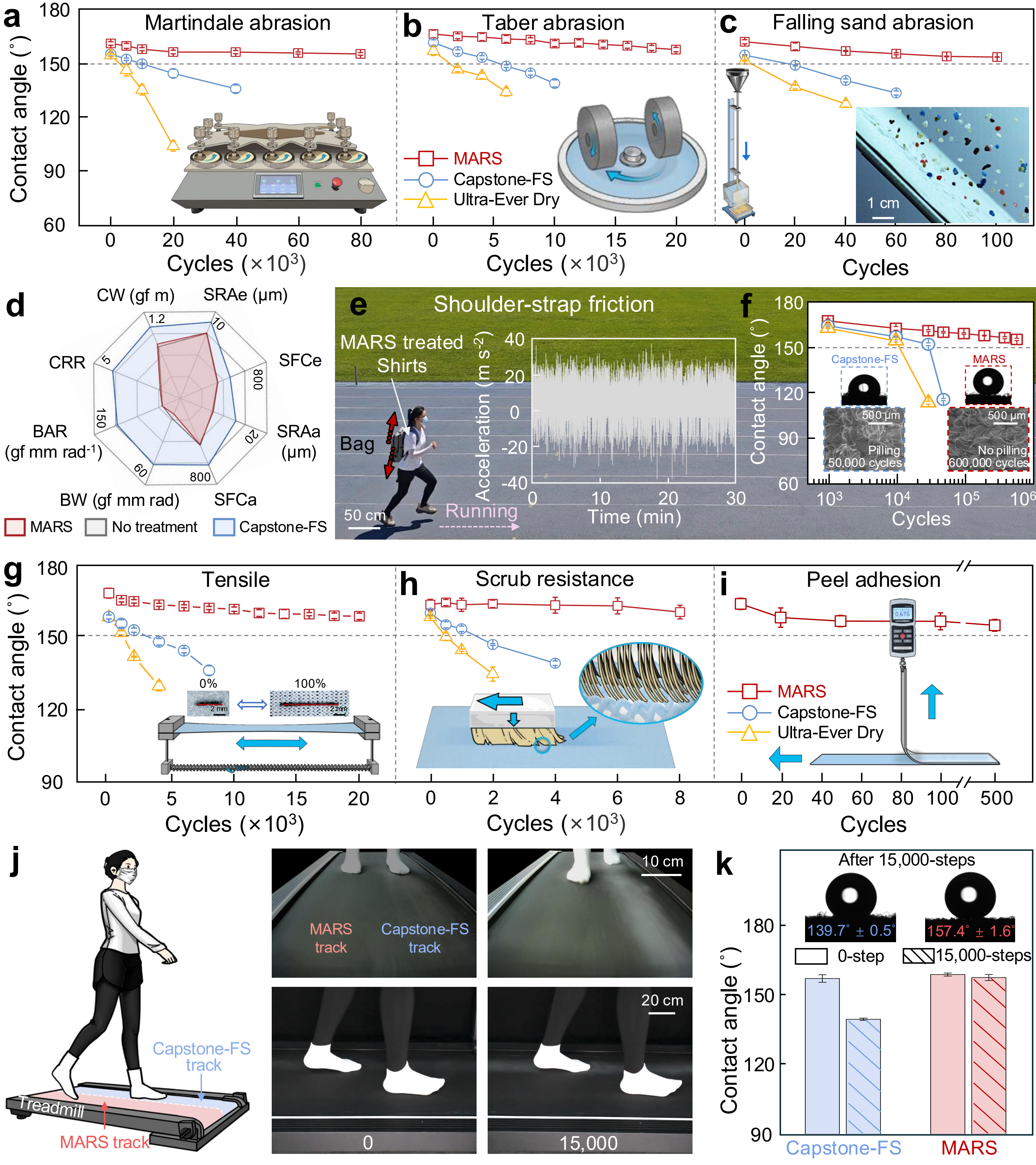
a
Martindale abrasion
Contact angle (˚)
Cycles (×10³)
b
Taber abrasion
Cycles (×10³)
MARS
Capstone-FS
Ultra-Ever Dry
c
Falling sand abrasion
1 cm
Cycles
d
CW (gf m)
SRAe (μm)
CRR
SFCe
BAR (gf mm rad⁻¹)
SRAa (μm)
BW (gf mm rad)
SFCa
1.2
10
5
800
150
20
60
800
MARS
No treatment
Capstone-FS
e
Shoulder-strap friction
MARS treated Shirts
Bag
50 cm
Running
Acceleration (m s⁻²)
Time (min)
f
Capstone-FS
MARS
500 μm
Piling 50,000 cycles
500 μm
No pilling 600,000 cycles
Contact angle (˚)
Cycles
g
Tensile
0%
100%
2 mm
2 mm
Contact angle (˚)
Cycles (×10³)
h
Scrub resistance
Cycles (×10³)
i
Peel adhesion
MARS
Capstone-FS
Ultra-Ever Dry
Cycles
j
Capstone-FS track
MARS track
Treadmill
MARS track
Capstone-FS track
10 cm
20 cm
0
15,000
k
After 15,000-steps
139.7˚ ± 0.5˚
157.4˚ ± 1.6˚
0-step
15,000-steps
Contact angle (˚)
Capstone-FS
MARS

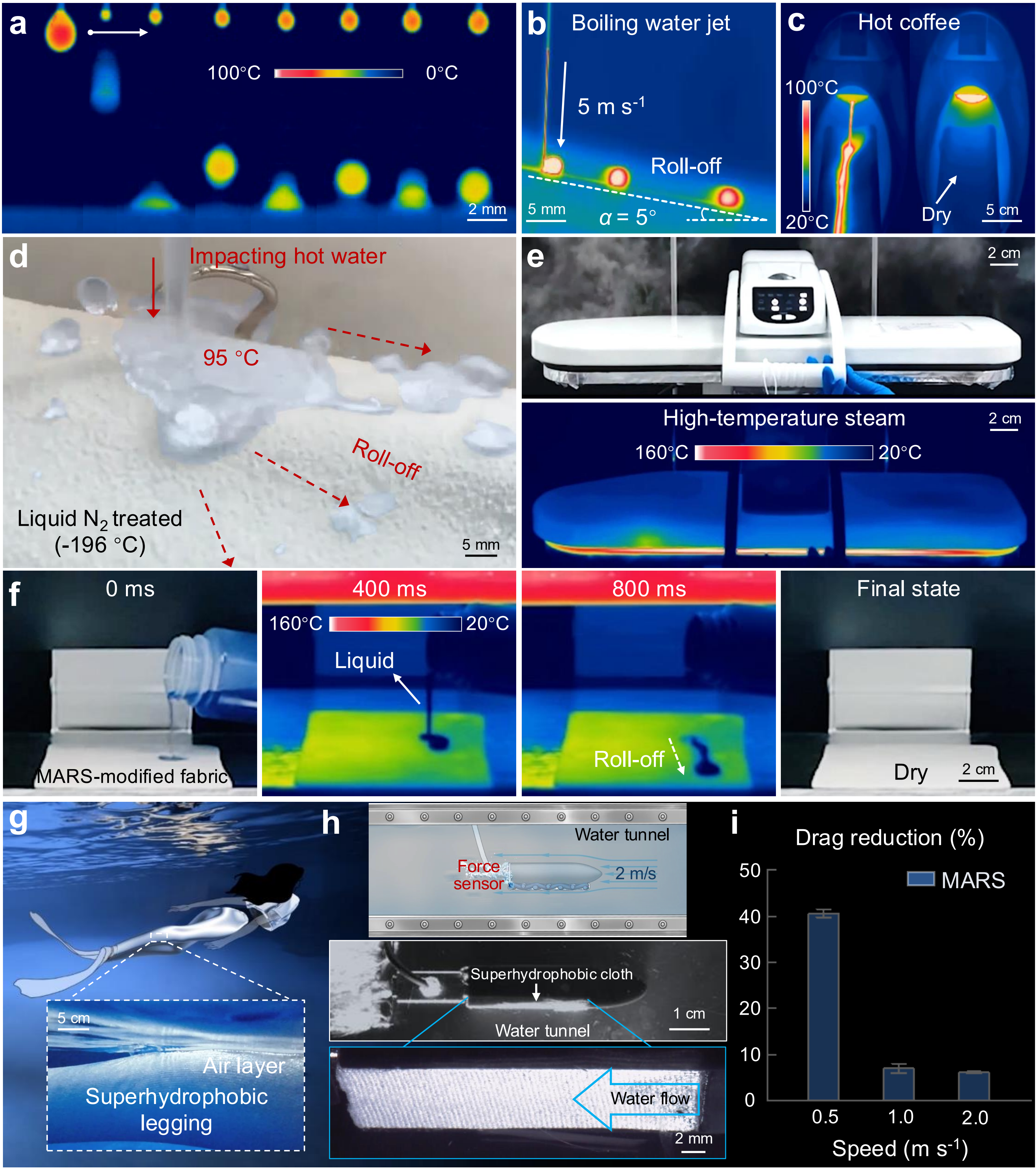
a
100°C
0°C
2 mm
b
Boiling water jet
5 m s^{-1}
Roll-off
5 mm
α = 5°
c
Hot coffee
100°C
20°C
Dry
5 cm
d
Impacting hot water
95 °C
Roll-off
Liquid N$_2$ treated
(-196 °C)
5 mm
e
2 cm
High-temperature steam
2 cm
160°C
20°C
f
0 ms
MARS-modified fabric
400 ms
160°C
20°C
Liquid
800 ms
Roll-off
Final state
Dry
2 cm
g
5 cm
Air layer
Superhydrophobic
legging
h
Water tunnel
Force
sensor
2 m/s
Superhydrophobic cloth
1 cm
Water tunnel
Water flow
2 mm
i
Drag reduction (%)
MARS
50
40
30
20
10
0
0.5
1.0
2.0
Speed (m s^{-1})